Available online at www.sciencedirect.com
SCIENCE DIRECT
Polymer 47 (2006) 3715–3726
polymer
www.elsevier.com/locate/polymer

Study of cationic UV curing and UV laser ablation behavior of coatings sensitized by novel sensitizers

Zhigang Chen, Dean C. Webster *

Department of Coatings and Polymeric Materials, Center for Nanoscale Science and Engineering, North Dakota State University, 1735 NDSU Research Park Drive, Fargo, ND 58105, USA

Received 23 August 2005; received in revised form 16 March 2006; accepted 23 March 2006
Available online 18 April 2006

Abstract

To improve the laser ablation performance of cycloaliphatic epoxide cationic UV curable coatings, two novel reactive sensitizers were synthesized and characterized and their effect on coating properties examined. The sensitizers were synthesized based on the reaction between naphthalene or anthracene derivatives and monomers or oligomers used in the coating system. HPLC and GC-MS confirmed the formation of the desired products. Three coating systems based on cycloaliphatic epoxide with either oxetane or polycaprolactone polyol were formulated with the reactive sensitizers. The sensitized coatings had higher conversion during UV curing in the oxetane containing formulation and did not deter the curing in the polyol containing formulation. Better UV laser ablation performance was observed in all sensitized coatings compared to the controls. Coatings with the anthracene based sensitizer even had better laser ablation performance than a commercial polyimide. The sensitized coatings had higher hardness, T_g and crosslink density while the adhesion and solvent resistance were not affected. An optimal amount of sensitizer was found for each coating formulation in terms of UV curing behavior. The relationship between coating T_g and laser ablation behavior was investigated and it was found that the higher the T_g and crosslink density, the poorer the laser ablation performance.

Keywords: Polymer materials; Laser ablation; Photopolymerization

1. Introduction

Cycloaliphatic epoxide based cationic UV curable coatings offer the advantage of fast cure, low shrinkage, no oxygen inhibition [1], and good electrical properties [2–4]. These characteristics make them ideal for microelectronics packaging materials. Due to the limited UV absorption of the onium salt cationic UV initiators using typical UV lamps, polynuclear aromatic compounds may be used as photosensitizers to extend the absorption of the system and subsequently to improve its UV curing rate and monomer conversion [5–8]. The sensitization is based on complex formation and electron transfer between the sensitizer and the photoinitiator [5,8]. Laser ablation is becoming more and more important as a material processing tool in the field of micromachining [9–11]. Many materials such as polyimide, polycarbonate and PMMA have been studied for laser ablation behavior [10–12]. The addition of a dopant such as pyrene or naphthalene is a common practice in aiding laser ablation [13,14]. The mechanism of laser ablation has been widely studied. Both pyrolysis and photolysis of the material are found to be involved [9,11,12,15], but which mechanism is predominant depends on both the laser source and material used [15,16]. At the beginning of ablation, a stage called incubation is commonly observed during which the less absorbent material is turned into a more absorbent intermediate upon the interaction with the energy delivered by incident laser light [10,11].

Flexible electronic devices such as displays or RFID tags are being proposed that consist of several layers of polymer containing embedded microchips. One possible method for constructing these multilayered devices is to apply and cure a cationic UV curable photopolymer onto an existing polymer substrate containing an integrated circuit. In order to provide pathways for interlayer connections, the polymer must be removed in specific locations to create vias. A convenient method is ablation using a high powered laser. Since, the cost of each photon is of most concern in laser processing [15], it is desired to reach the designated via dimension with the least number of laser photons; also, debris in the ablation spot and surrounding area should be minimized. On the other hand, no

* Corresponding author. Tel.: +1 701 231 8709; fax: +1 701 231 8439.
E-mail address: dean.webster@ndsu.edu (D.C. Webster).

0032-3861/$ - see front matter © 2006 Elsevier Ltd. All rights reserved.
doi:10.1016/j.polymer.2006.03.091

research has been reported on laser ablatable cationic UV curable coatings. Thus, research in this area is considered to be important from both the academic and practical application point of view. Previously it was found by our group that the addition of monomeric pyrene into cycloaliphatic epoxide/difunctional oxetane/sulfonium salt based cationic UV curable coating greatly enhanced the laser ablation depth of the coating, but the curing time doubled from 30 to 60 s [17]. The deterred curing was attributed to the incompatibility between monomeric pyrene and the host coating such that the UV energy absorbed by pyrene cannot be utilized to sensitize the photoinitiator since the chance of complex formation between pyrene and photoinitiator is low. As a result, the net UV energy that reaches photoinitiator is reduced, consequently causing slower curing of the coating. A solution to this dilemma is to design and synthesize an additive for a cationic UV curable system that enhances UV laser ablation without deterring UV curing. In this paper, we describe such a strategy. Further, it is believed that the material absorption of the incident laser energy is most important for successful laser ablation [9,15]. Since the ablation laser wavelength is 355 nm in the aforementioned application, we focused on naphthalene and anthracene derivatives instead of pyrene in this work due to their stronger absorption around 355 nm [18,19].

2. Experimental section

2.1. Materials

Cyracure™ UVR 6110 difunctional cycloaliphatic epoxide (3,4-epoxycyclohexylmethyl-3-4-epoxycyclohexane carboxylate, ECC), UVR 6000 monofunctional reactive oxetane diluent (3-ethyl-3-hydroxymethyl oxetane, EHMO), Tone™0301(ε-caprolactone polyol, PCL) flexibilizer, and UVI 6974 photoinitiator (mixed triarylsulfonium hexafluoroantimonate salt in propylene carbonate, PI) were obtained from Dow Chemical Company. Difunctional oxetane reactive diluent OXT-221 (bis{[1-ethyl(3-oxetanyl)]methyl} ether, DOX) was provided by Toagosei Co. Ltd, AMBERLYST® 15 ion-exchange resin with sulfonic acid functionality (A15), AMBERLYST® A-21 ion-exchange resin with alkyl tertiary amine functionality (A21), naphthalene dicarboxylate (NDC) and 9-anthracene carboxylic acid (ACA) were obtained from Aldrich. All materials were used as received.

2.2. Synthesis of novel reactive sensitizers

Scheme 1 shows the synthesis routes for the two novel reactive sensitizers. Reactions were carried out in a 100 ml three neck flask equipped with nitrogen inlet, reflux condenser and magnetic stirrer. The reaction temperature was maintained by a heating mantle and a thermocouple linked to a temperature controller. The reaction mixture was dried in a vacuum oven (30 mmHg, ~65 °C) before characterization and use. The transesterification reaction of NDC and EHMO (Reaction A, Scheme 1) was accomplished by adding 6.11 g NDC, 5.80 g EHMO (mole ratio = 1:2), 1.77 g A21 and 30 g xylene into the reaction flask. The reaction temperature was kept at 100 °C for 24 h with nitrogen purge. The product is abbreviated as NDC-OX. The esterification reaction of ACA and PCL (Reaction B, Scheme 1) was accomplished by adding 1.11 g ACA, 1.50 g PCL (mole ratio = 1:1), 0.1 g A15 and 20 g xylene into reaction flask. The reaction temperature was kept at 120 °C for 29 h with nitrogen purge. The product was abbreviated as ACA-OL.

2.3. Characterization of reactive sensitizers and sensitized coatings

High performance liquid chromatography (HPLC) analysis was performed on an Agilent 1100 series HPLC utilizing a diode array detector (DAD) for UV–Vis characterization. Chromatographic separation was achieved on a reversed-phase ZORBAX C8 column (Agilent) with a C4 guard column (Thermo Electron). The mobile phase consisted of two solvents: solvent A (0.05 M ammonium phosphate, pH unadjusted) and solvent B (methanol). Column temperature was maintained at 40 °C throughout the analysis. A 15 μl injection volume was used for all samples. The column was eluted with the following gradient: 0 min, 35% B; 18 min, 35% B; 18.1 min, 85% B; 28 min, 85% B; 28.10 min, 35% B. Flow rate was 0.7 ml/min with a 40 min runtime per injection. GC-MS analysis was performed using a HP 6890 gas

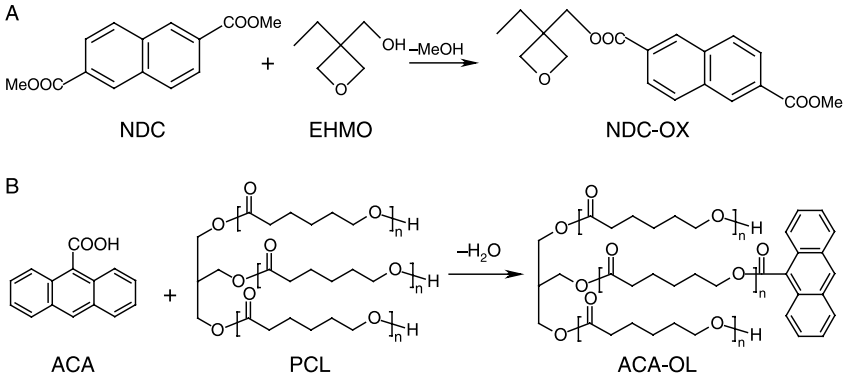

Scheme 1. Synthesis routes of the reactive sensitizers: (A) synthesis of NDC-OX by transesterification of NDC and EHMO. (B) Synthesis of ACA-OL by esterification of ACA and PCL.

chromatograph and HP 5973 mass selective detector utilizing EI (electron ionization) with filament energy of 69.9 keV. The initial GC oven temperature was 70 °C, then it was ramped up to 300 °C at a rate of 20 °C/min. The front inlet was in split mode with inlet temperature 250 °C and pressure 8.24 psi. The split ratio and the run time (normally 1 h) varied with the different samples. Separation was achieved on a ZEBRON ZB-35 capillary column operated in a constant flow mode with flow rate of 1.0 ml/min; the average velocity is 36 cm/s. The mass spectrometer was in scan mode with m/z ranges from 10 to 800, the temperature for MS source and MS Quad were set at 230 and 150 °C, respectively.

Coating films were prepared by casting the liquid sample onto an aluminum panel or a polysulfone film (thickness ~130 μm) with a Gardco 70# wire drawdown bar. The cured coating film had a thickness of 90–120 μm, measured using a Micromaster® micrometer, which was much thicker than the typical thickness of UV curable coatings (10–20 μm). By using this unusually high film thickness it is possible to monitor the laser ablation of the coating film as a function of increasing laser pulses. A problem accompanying the thicker coating film was the curling on the polysulfone substrate due to internal stress generated during UV curing, but when the cured film thickness was reduced to around 20 μm, a flat film was achieved. UV curing of coating samples was performed using a Dymax light source with a 200 EC silver lamp (UV-A, 365 nm) in air; light intensity was 35 mW/cm^2 measured by NIST Traceable Radiometer, International Light model IL1400A.

Photoinfrared experiments were performed using a Nicolet Magna-IR 850 Spectrometer Series II with detector type DTGS KBr, and a UV optic fiber mounted in a sample chamber in which humidity was kept around 20% by Drierite®. The light source was a LESCO Super Spot MK II 100 W DC mercury vapor short-arc lamp. Such setup monitors the reactive functional group conversion as the photo reaction proceeds and is known as real-time infrared spectrometry (RTIR). Coating samples were spin coated onto a KBr plate at 3000 rpm for about 15 s, which were then exposed to UV light for 60 s. Scans were taken over a 120 s period at 2 scans/s. The UV intensity was adjusted to ~3.6 mW/cm^2 and the experiment was performed in air. The average standard deviation for the RTIR measurements is approximately ±2%. The oxirane conversion of ECC was monitored at 789 cm^{-1} and the oxetane conversion of EHMO and DOX was monitored at 976–977 cm^{-1}. The average conversion at 120 s is presented.

Dynamic mechanical thermal analysis (DMTA) was accomplished using a Rheometric Scientific 3E apparatus in the rectangular tension/compression geometry. The cured coating film was removed from the polysulfone substrate using a razor blade; the sample size for testing was 10×5 mm^2. The analysis was carried out from 0 to 250 °C at a frequency of 10 rad/s and a ramp rate of 5 °C/min. T_g was obtained from the maximum peak in the tan δ curves, crosslink density (ν_e) was calculated according to equation: $E' = 3\nu_e RT$, where E' value was determined in the linear portion at least 50 °C greater than the T_g.

Hardness testing was performed with a BYK Gardener pendulum hardness tester in the König mode on an aluminum panel; cross-hatch adhesion test was performed on polysulfone substrate using a Gardco cross-hatch cutter which creates a 5× 5 pattern of squares. Adhesive tape was then applied onto the pattern and was pulled off, followed by a visual examination of coating loss. Methyl ethyl ketone (MEK) double rub experiment was used to assess the solvent resistance of the coatings. Coating samples were applied onto aluminum panels, UV cured and kept at room temperature for 1 h before testing. A 26 ounce hammer with five layers of cheesecloth wrapped around the hammerhead was soaked in MEK for rubbing. After 100 double rubs the cloth was rewet with MEK. The number of double rubs was reported as the point where mar appeared on the film surface, or a maximum of 400 double rubs was recorded.

UV laser ablation of cured coating films on polysulfone substrate was done using a Nd:YAG (Neodymium–doped Yttrium Aluminum Garnet) laser. Laser parameters were: wavelength 355 nm, power 0.2 W, effective laser beam spot size 40 μm, beam spiral diameter 200 μm, velocity 125 mm/s, repetition rate 20 kHz. For each sample film, a 16-via array as shown in Fig. 1 was generated. The number under each array represents laser pulses used to create the respective array. Nitrogen flow over the film surface was used to carry away ablation debris.

A Wyko NT3300 Optical Profiler from VEECO was used to obtain profile data of vias created by laser ablation. VSI (vertical scanning interferometry) mode and a magnification of 50×0.5 were used. Back scan length was set at 20 μm, scan length was varied from 100 to 250 μm as pulses increases. Vision 32 for NT-2000 software, version 2.303 was used to process the profiler data. Only the center four vias were selected for measurement. The average standard deviation of this measurement is ca. ±4 μm. UV–Vis spectra of the coating films were obtained using a Varian Cary 5000 UV–vis–NIR spectrophotometer operating in absorption mode. The scanning rate was 600 nm/min and scanning range was 200–600 nm. The coating was applied and UV cured on quartz slide with film thickness between 20 and 24 μm for UV–Vis experiments.

Three different cationic UV curing formulation systems (ECC-EHMO, ECC-DOX and ECC-PCL) were formulated based on ECC and three commonly used reactive diluents, EHMO, DOX and PCL. The coating formulations studied are

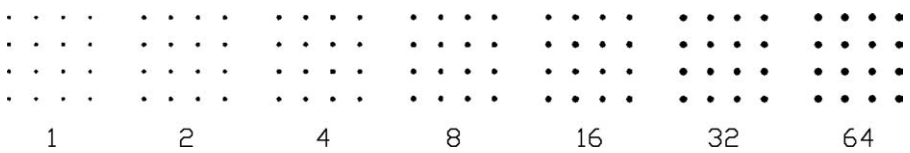

Fig. 1. Via arrays created by 355 nm YAG laser ablation on cationic UV curable coatings. The number below each array represents the laser pulses used.

Table 1
Formulations of cationic UV curable coatings studied in this work

System	Formulations	Materials (wt%)					
		ECC	PI	EHMO	DOX	PCL	Sensitizer (0.1 mmol/5 g coating)
A. Sensitized and blank coating formulations							
ECC-EHMO	Blank	70	4	25	0	0	None
	+NDC-OX						NDC-OX
	+ACA-OL						ACA-OL
ECC-DOX	Blank			0	25	0	None
	+NDC-OX						NDC-OX
	+ACA-OL						ACA-OL
ECC-PCL	Blank			0	0	25	None
	+NDC-OX						NDC-OX
	+ACA-OL						ACA-OL
B. Formulations with T_g variation							
ECC-EHMO	Mid T_g	70	4	15	10	0	None
	Mid T_g+NDC-OX			15	10		NDC-OX
	High T_g			5	20		None
	High T_g+NDC-OX			5	20		NDC-OX
ECC-PCL	Mid T_g	80		0	0	15	None
	High T_g	90				5	None

given in Table 1A and B. Due to the different functionality/reactivity of the diluents and the roles they play during the UV curing process, these coating systems were expected to exhibit quite different curing reactivity and film properties such as T_g, hardness and crosslink density. System ECC-DOX was expected to be highly reactive and crosslinked because of the two reactive oxetane functionalities in DOX, while system ECC-PCL will tend to be less crosslinked and more flexible due to the presence of PCL. As to system ECC-EHMO, the addition of a mono functional oxetane diluent was expected to give coating properties between system ECC-DOX and ECC-PCL. Reactive sensitizers were added into the coating formulation with the ratio of 0.1 mmol/5 g coating (~1% wt, theoretical MW of the sensitizers are used for calculation) for each coating system. By systematically examining the properties (including laser ablation sensitivity) of these sensitized coatings, it was hoped to better understand the effect of the reactive sensitizers on coating matrixes having widely varying properties.

3. Results and discussion

Due to limited absorbance at the incident UV laser ablation wavelength of 355 nm, UV cured cycloaliphatic epoxy coatings have poor laser ablation performance. The key to having a UV laser ablatable cationic UV curable coating—a system where UV curing is not deterred—is to identify a suitable polynuclear aromatic type additive.

3.1. Effect of non-modified sensitizer

In order to address the solubility issue encountered when using monomeric pyrene, 9-anthracene carboxylic acid (ACA) was chosen as an alternative. It was thought that ACA should have better solubility in the coating systems due to the existence of hydrogen bonding; furthermore, as an acid and proton donor, it was expected to aid the photo induced super acid generation in the initiation stage [20]. ACA (0.0222 g, 0.1 mmol) was added into 5 g ECC-EHMO and ECC-PCL formulations and were named ECC-EHMO + ACA and ECC-PCL + ACA, respectively. The ACA sensitized samples were heated at 50 °C for about 30 min in order to dissolve ACA; the RTIR result is shown in Table 2. Deterred curing (lower monomer conversion than the blank sample) for these samples was again observed and attributed to not enough solubility in the coating matrix.

3.2. Synthesis and characterization of novel reactive sensitizers

The chemical modification of monomeric polynuclear aromatic sensitizers is an effective way to enhance their solubility in the coating and lower their vapor pressure and toxicity [5]. It was thought that a straightforward approach for this would be the attachment of the polynuclear aromatic compounds to the coating ingredients such as the reactive diluents. Due to the similarity effect, the resultant sensitizer was expected to have good compatibility/solubility in the coating matrix. Also, since they are reactive and bound to the crosslinked coating network during the photopolymerization process, any potential sensitizer migration is eliminated. Based on this concept, two reactive sensitizers were synthesized as

Table 2
Cycloaliphatic epoxide and oxetane conversion in RTIR experiments for ACA sensitized coatings

Formulations		Epoxide conv. (%) at 120 s	Oxetane conv. (%) at 120 s
ECC-EHMO	Blank	46	69
	+ACA	23	26
ECC-PCL	Blank	74	–
	+ACA	69	–

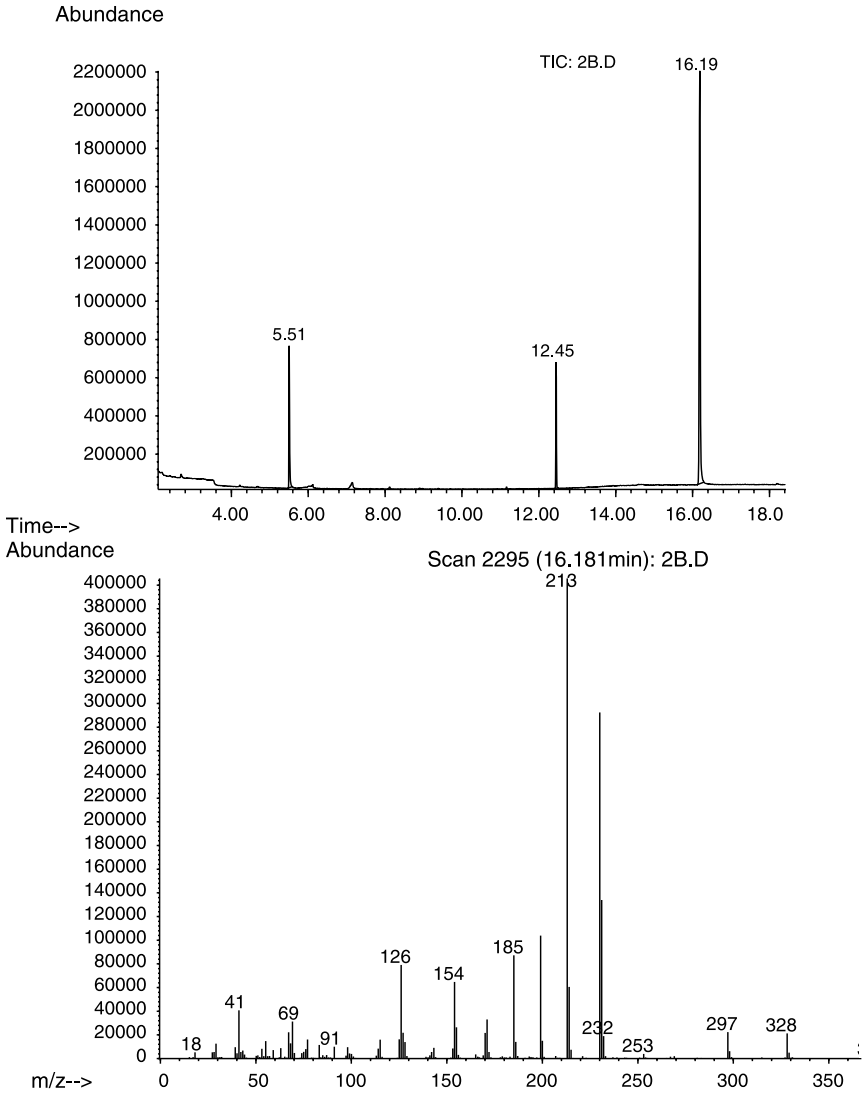

Fig. 2. GC chromatogram (upper) and MS spectrum (lower) for NDC-OX.

shown in Scheme 1. The formation of the desired products was confirmed by HPLC and GC-MS as described below:

NDC-OX is a white powder soluble in acetone and chloroform; formation of it was confirmed by GC-MS as shown in Fig. 2. The 5.51 and 12.45 min peaks in GC chromatogram (upper) are unreacted EHMO and NDC, respectively, the 16.19 min peak is NDC-OX (MW 328) with its molecular ion showing in the MS spectrum (lower). The reaction product is estimated to contain ~71.8% NDC-OX by peak area integration in the GC chromatogram.

ACA-OL (MW 522) is a yellowish paste. GC-MS did not show any new product peaks except for the peaks of ACA and PCL, while HPLC analysis indicates the formation of target product. Fig. 3(a) and (b) show the HPLC chromatogram of the reaction product mixture and UV–Vis absorption spectra of the target product, PCL, and ACA. The two peaks at ~15 min in the HPLC chromatogram belong to unreacted ACA. All the peaks after 20 min have a different UV absorption spectrum from that of both ACA and PCL and they have the characteristic UV absorption between 330 and 390 nm of ACA, indicating the attachment of ACA to the polyol. The reaction product mixture is estimated to contain ~49.5% ACA-OL by peak area integration. The sensitizer NDC-OX and ACA-OL were expected to be "reactive" since the oxetane group in NDC-OX will take part in the photopolymerization, and the polyol moiety in ACA-OL will be incorporated into the network via chain transfer reaction [21]. The reaction products were put into the coating formulations after removing the catalyst and solvent. No further separation/purification of the reaction product mixture was carried out since a sufficient amount of monomeric polyaromatic compounds had been modified according to the spectroscopic data. As to the unreacted reactants, the trace amount of EHMO, NDC and PCL brought in by ~1 wt% NDC-OX and ACA-PCL are negligible. In addition, the ACA was shown earlier to have a negative effect on photopolymerization of the sensitized coatings as a result of its poor solubility in the coating matrix. So in terms of photopolymerization of the sensitized coatings, any enhancement in monomer conversion should be attributed to the synthesized reactive sensitizers, while all the polynuclear

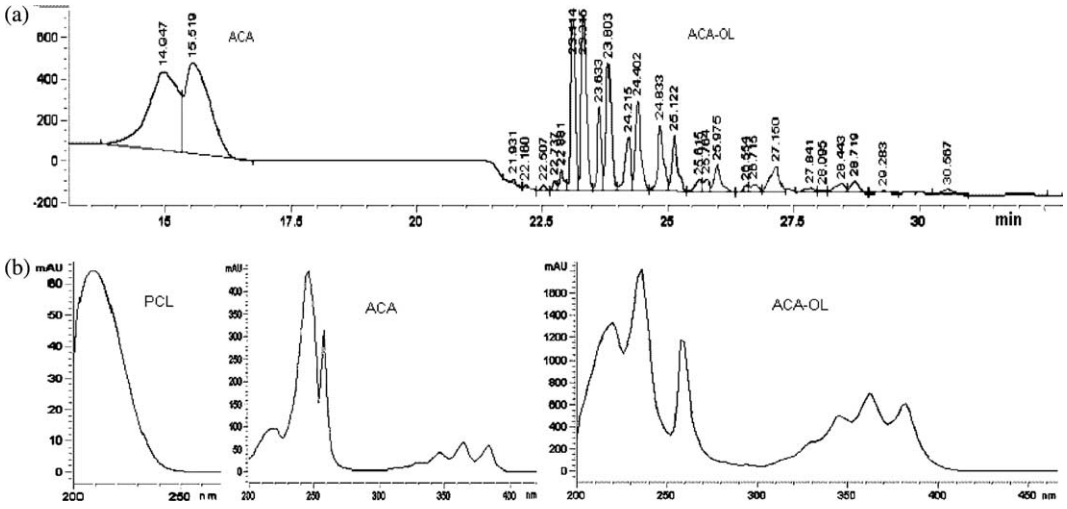

Fig. 3. HPLC chromatogram and UV–vis spectrum for ACA-OL: (a) HPLC chromatogram for reaction product of ACA and PCL. (b) UV absorption spectra for PCL, ACA and ACA-OL.

aromatic compounds were expected to be effective laser ablation sensitizers.

3.3. Effect of reactive sensitizers

The synthesized sensitizers—NDC-OX and ACA-OL—were added into the formulations ECC-EHMO, ECC-DOX and ECC-PCL to examine their sensitization effect. The sensitizers dissolved in the coating after being heated at ~50 °C for about 15 min on a hot plate with frequent shaking; the sensitized coating samples were clear liquids at room temperature. These sensitized samples were characterized along with the blank formulations to examine the effect of the sensitizers on the properties of the different coating matrixes.

3.3.1. Photopolymerization of sensitized coatings

The effect of the reactive sensitizers on the curing behavior of cationic UV curable coatings was studied. Table 3 shows the RTIR reactive functional group conversion data for ECC-EHMO, ECC-DOX and ECC-PCL formulation systems. First, it is noted that none of the sensitized coatings exhibited deterred UV curing. On the contrary, they exhibit, to varying degrees, a photosensitization effect as the result of improved solubility/compatibility in the coating matrix. Furthermore, it is apparent that the magnitude of the photosensitization effect is closely related to the mobility of the formulation system. For example, in the system ECC-EHMO, all of the sensitized coating samples exhibit pronounced higher reactive functional group conversion than the blank formulation, especially in the case of oxetane conversion. In the system ECC-DOX, the sensitization effect is less pronounced. The difference between systems ECC-EHMO and ECC-DOX can be attributed to mobility factors. In comparison to the system ECC-EHMO, system ECC-DOX is a highly reactive and crosslinked one in which the vitrification point is earlier than system ECC-EHMO. Since, effective sensitization depends on collision, complex formation and electron transfer between the sensitizer and initiator molecules [5], a 'rigid' system like ECC-DOX would 'freeze' the molecules early so that the sensitization interaction is restrained. As to system ECC-PCL, the mobility provided by the large amount of polyol is the highest. Also, as a chain transfer agent, the polyol helps to boost the monomer conversion rate [21-23]. As a result, the cycloaliphatic epoxide conversion is already high so that sensitizers play a less important role in the photo curing process. These factors account for the similar curing behavior observed in

Table 3
Cycloaliphatic epoxide and oxetane conversion in RTIR experiments for NDC-OX and ACA-OL sensitized coatings

Formulations		Epoxide conv. (%) at 120 s	Oxetane conv. (%) at 120 s
ECC-EHMO	Blank	46	69
	+NDC-OX	58	76
	+ACA-OL	61	88
ECC-DOX	Blank	44	65
	+NDC-OX	43	69
	+ACA-OL	51	67
ECC-PCL	Blank	74	–
	+NDC-OX	80	–
	+ACA-OL	79	–

Table 4
Cycloaliphatic epoxide and oxetane conversion in RTIR experiments for coatings sensitized by varied amount of NDC-OX

Formulations		Epoxide conv. (%) at 120 s	Oxetane conv. (%) at 120 s
ECC-EHMO	Blank	46	69
	Half (0.05 mmol)	57	81
	+NDC-OX (0.1 mmol)	58	76
	Double (0.2 mmol)	15	15
	Triple (0.3 mmol)	26	32
ECC-PCL	Blank	74	–
	Half (0.05 mmol)	57	–
	+NDC-OX (0.1 mmol)	80	–
	Double (0.2 mmol)	78	–
	Triple (0.3 mmol)	76	–

Table 5
Thermal and mechanical properties of NDC-OX and ACA-OL sensitized coatings in comparison with blank samples in three formulation systems

Film properties /formulations	ECC-EHMO			ECC-DOX			ECC-PCL		
	Blank	NDC-OX	ACA-OL	Blank	NDC-OX	ACA-OL	Blank	NDC-OX	ACA-OL
Film thickness (μm)	90	110	120	100	110	90	90	110	90
X-hatch adhesion		25/25			25/25			25/25	
MEK double rub (cycles)		>400, no mar			>400, no mar		50	100	50
Pendulum hardness (s)	197	213	220	Not measured	195	196	194		
Curling		Slight			Serious			Very slight	
DMTA T_g (°C)	135.5	149.0	145.4	167.1	161.0	150.2	93.60	103.4	91.98
ν_e ($\times$mmol/cm^3)	8.203	9.962	10.38	22.13	27.84	21.45	2.420	2.580	2.811

formulations of system ECC-PCL. This explanation is further validated by the crosslink density data of these three formulation systems as shown in Table 5, which will be discussed later.

The amount of NDC-OX in systems ECC-EHMO and ECC-PCL was also varied in order to study the effect of the sensitizer amount on photo curing. The RTIR results are shown in Table 4, where 'half, double and triple' denotes that the amount of NDC-OX in the formulation is half, double and triple of 0.1 mmol/5 g, respectively. Within the studied variation range, it is seen that the maximum reactive functional group conversion is achieved when the NDC-OX is added at 0.05–0.1 mmol for system ECC-EHMO, and around 0.1 mmol for system ECC-PCL. The reason for this optimal photosensitizer amount could be that there exists an optimal photoinitiator–photosensitizer ratio in each of the coating systems. Given that the amount of photoinitiator is fixed in the coatings, if the amount of photosensitizer is too low, then part of the photoinitiator cannot be sensitized which results in lower reactive functional group conversion. On the other hand, if the amount of photosensitizer is too high, then the excess photosensitizer will only serve as a UV energy absorber, consequently preventing the deeper part of the coating from absorbing the UV energy.

3.3.2. Mechanical and thermal properties of the sensitized coatings. The mechanical and thermal properties of the sensitized coatings were characterized and the results are summarized in Table 5. All of the formulations have excellent adhesion to the polysulfone substrate. System ECC-EHMO and ECC-DOX samples have excellent solvent resistance due to their higher crosslink density. As to system ECC-PCL samples, the poor solvent resistance is attributed to the large amount of polyol, which not only decreases the molecular weight of the

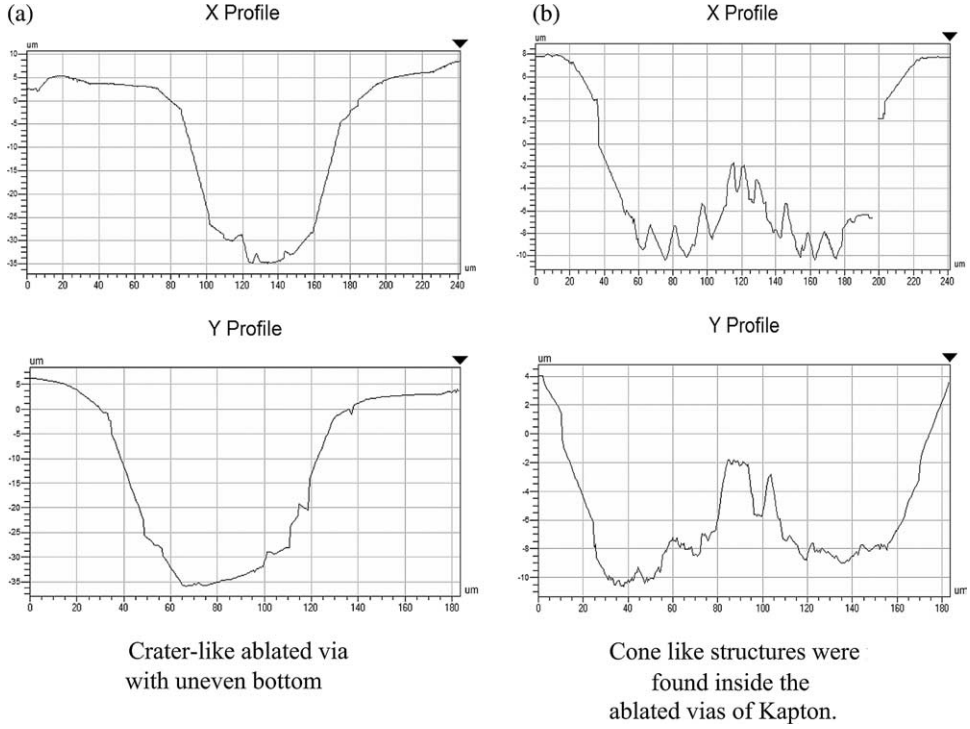

Fig. 4. 2D profile of laser ablation vias obtained from optical profiler.

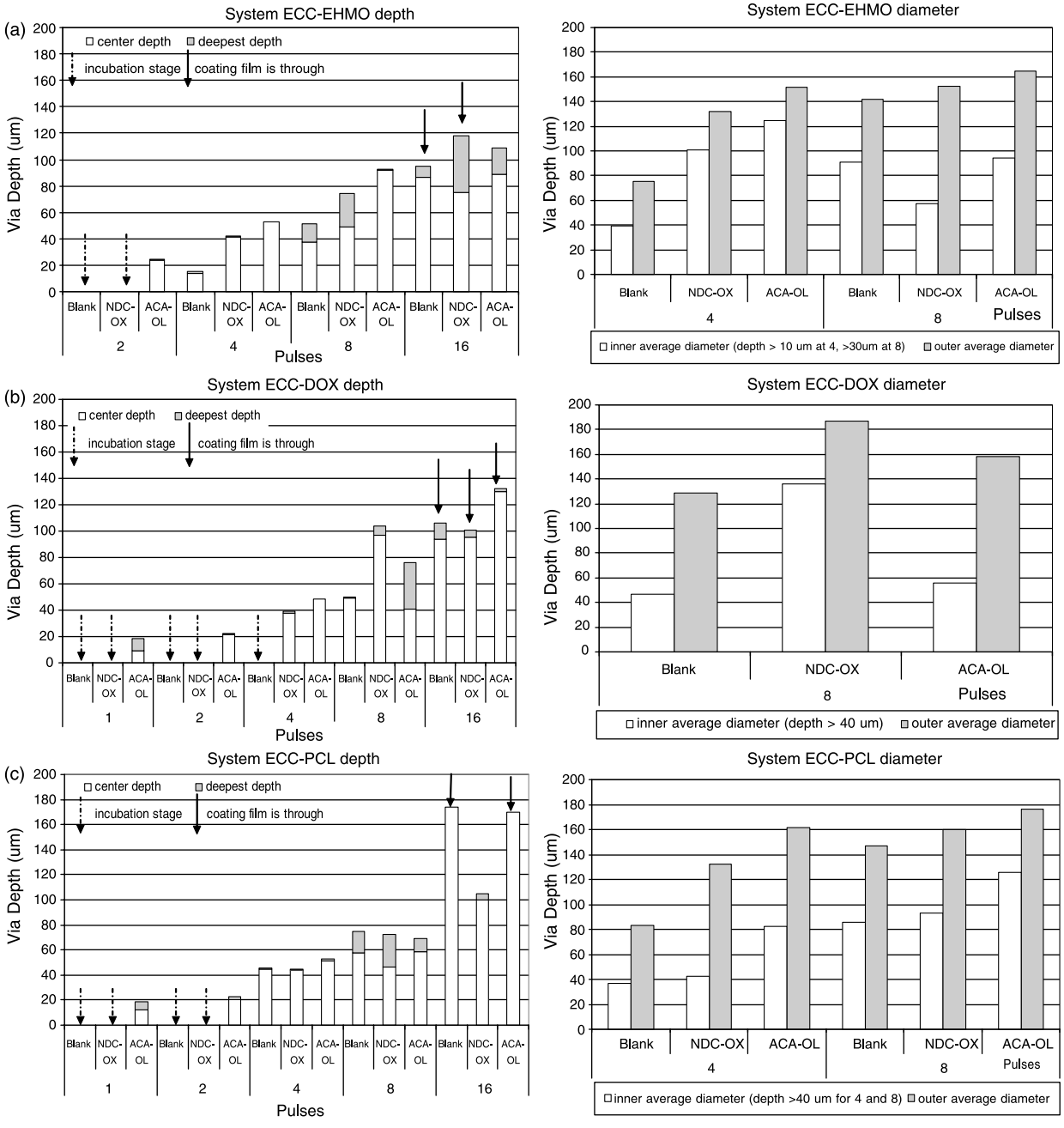

Fig. 5. Comparison of depth (left) and diameter (right) of vias created by laser ablation in different formulation systems: (a) ECC-EHMO formulations; (b) ECC-DOX formulations; (c) ECC-PCL formulations.

photo crosslinked polymer as a chain transfer agent [18,21], but also is susceptible to solvent attack due to its linear structure. For the DMTA data, higher T_g and ν_e are observed for sensitized samples in system ECC-EHMO, which correlates well with the higher monomer conversion observed in the RTIR experiment. Consequently, the hardness is also higher. As to systems ECC-DOX and ECC-PCL, much less pronounced photosensitization was observed in the photo curing process, thus not much variation was noticed in the mechanical properties. The curling of the cured film on polysulfone substrate seems to correlate well with the crosslink density. Due to the higher functionality and reactivity of system ECC-DOX, all of its samples exhibit serious curling, compromising their potential in practical applications.

3.3.3. Laser ablation of sensitized coating films. The profile data of the vias created by UV laser ablation on UV cured coating films and two reference films, Kapton (polyimide) and PEN (polyethylene naphthalene), were obtained from the profilometer and processed in Vision 32 for NT-2000 software as shown in Fig. 4. Vias of the coating films and PEN have a crater-like profile with an uneven bottom as shown in Fig. 4a. Vias of Kapton are different. Cone-like structures were found in the vias at all pulses and were attributed to impurities [15].

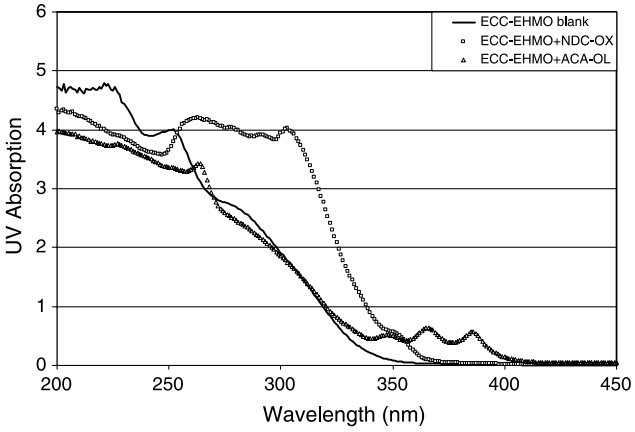

Fig. 6. UV–vis absorption spectra for blank and sensitized coating films in system ECC-EHMO.

The dimension data of ablated vias are shown in Fig. 5, where the deepest depth was obtained from a 'filtered histogram' analysis tool provided by the software, and the inner average diameter was obtained by averaging the *x* and *y* diameter below a certain depth. The dashed line arrows in Fig. 5 indicate that the sample is in the incubation stage [10,11], while the solid line arrows indicate that a through hole is ablated in the coating film.

From Fig. 5, it is noticed that even the addition of a small amount of reactive sensitizer (~1 wt%) greatly enhances the laser ablation of the coating films, especially at the initial several pulses (1, 2 and 4 pulses). But when the films were ablated by more pulses, the difference between sensitized and blank samples is less apparent since the effect of the sensitizer is probably overwhelmed by the high laser energy input. The effect of the reactive sensitizers is manifest in three aspects: (1) ablation starts earlier. This is observed at one and two pulses for all formulation systems, particularly for ACA-OL sensitized coatings. (2) The ablation depth is deeper at the same number of pulses. For system ECC-EHMO and ECC-DOX, at the number of pulses where all the samples begin to be ablated (pulses 4 and 8 for system ECC-EHMO and ECC-DOX, respectively), the ablation depth for the sensitized coatings reaches 40–50 μm, which is almost twice that of the blank sample. Given that a coating film typically has a thickness of 20 μm, this ablation result translates to higher ablation efficiency on ACA-OL sensitized coatings: when a through-hole is already ablated in the ACA-OL sensitized coating, the ablation on other coating samples has not even started. As to system ECC-PCL, the depth improvement is less, which can be explained by the lower polymer molecular weight and higher mobility inside the cured film as a result of the addition of large amount of polyol [15,23], thus even the blank sample can be ablated easily. (3) The inner and outer diameters of the ablated vias are larger. Since, the spiral diameter of the laser beam is 200 μm, a via having an outer diameter closer to 200 μm is considered to be better ablated. Fig. 5 shows that at the same pulse, the sensitized coatings have a larger diameter than the blank sample. Furthermore, at four pulses for system ECC-EHMO and ECC-PCL, the ACA-OL sensitized samples have diameters double that of the blank sample, showing a more pronounced sensitization effect. It is concluded from the results shown in Fig. 5 that ACA-OL sensitized coatings have better 355 nm laser ablation performance, which is attributed to the broader and stronger absorption around 355 nm shown in Fig. 6.

3.3.4. Comparison of ACA-OL sensitized coatings with Kapton and PEN for laser ablation. Kapton (polyimide) and poly(ethylene naphthalene) (PEN) films (with film thicknesses of 75 and 125 μm, respectively) were chosen as references in laser ablation experiments. They were ablated under the same conditions as the sample films for comparison. Kapton is a standard commercial material having good laser ablation properties, for which the ablation process is mainly based on a thermal mechanism [11,15]. PEN was expected to have good ablation performance due to the high content of UV

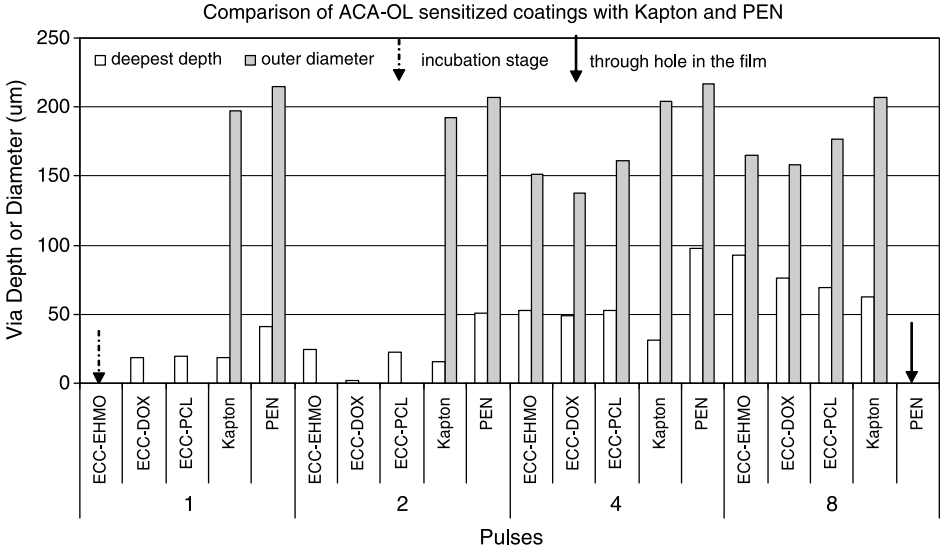

Fig. 7. Comparison of dimension data of laser ablated vias of Kapton and PEN with ACA-OL sensitized coatings.

Table 6
Thermal and mechanical properties of coatings with T_g variation

Film properties/ formulations	ECC-EHMO					ECC-PCL		
	Blank	Mid T_g	Mid T_g+ NDC-OX	High T_g	High T_g+ NDC-OX	Blank	Mid T_g	High T_g
Film thickness (μm)	90	110	80	90	90	90	110	110
X-hatch adhesion			25/25				25/25	
Curling	Slight	Medium	Medium	Serious	Serious	Very Slight	Medium	Medium
DMTA T_g (°C)	135.5	142.4	145.2	145.4	154.9	93.59	125.7	140.4
ν_e (×mmol/cm^3)	8.203	11.36	15.74	20.99	17.36	2.420	3.542	5.012

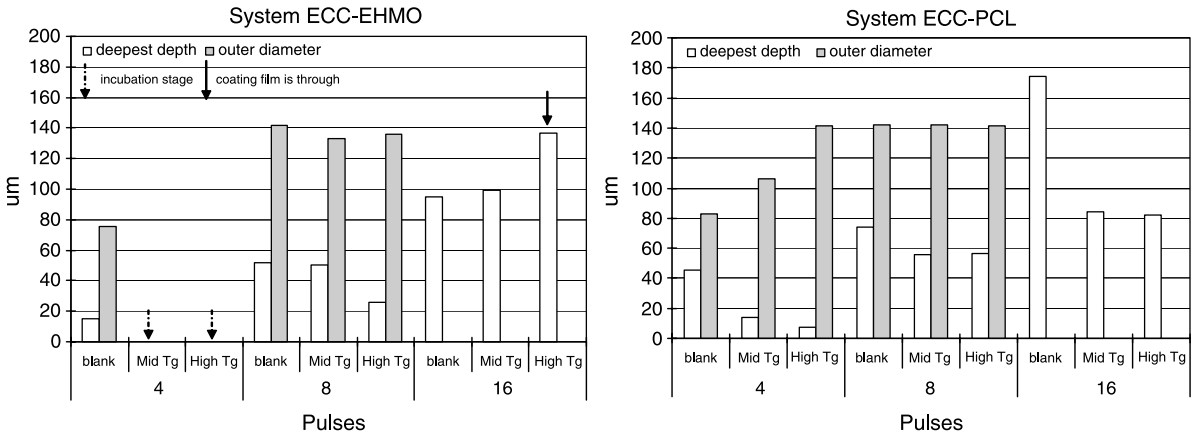

Fig. 8. Effect of T_g on ablation via dimension in system ECC-EHMO (left) and ECC-PCL (right). Diameter at 16 pulses was not measured.

absorbing naphthalene units in the polymer backbone. The ACA-OL sensitized coating samples were chosen for comparison with Kapton and PEN because of their better ablation performance over NDC-OX sensitized ones. Considering the cone-like structure inside the ablated vias of Kapton as shown in Fig. 4, only the deepest depth and outer diameters of the ablated vias (the outer diameters of coating samples were measured at four and eight pulses) were compared. The comparative results are shown in Fig. 7, from which it is apparent that the laser ablation performance of PEN is much better than all the materials studied as evidenced by its much deeper depth and larger diameter. As to ACA-OL sensitized coating samples and Kapton, the coating samples have deeper ablation depth than Kapton, but their outer diameters are much smaller than both Kapton and PEN, for which ~200 μm outer diameters were immediately reached after the first pulse. The coating samples seem to be less sensitive to the surrounding energy of the incident laser beam.

3.4. Effect of T_g on laser ablation

T_g is one of the most important properties of a polymer and is related to many other polymer properties. It has been found that polymers with a crosslinked structure or with higher molecular weight are more difficult to be ablated due to their higher stability and viscosity [15]. No report on the relationship between the T_g of a crosslinked polymer and its laser ablation behavior has been found. To investigate this relationship, a series of samples with T_g variation were designed as shown in Table 1B, where the T_g of the coating was varied by changing the percentage of difunctional monomers in the formulations. NDC-OX was added to system ECC-EHMO in order to further examine the effect of reactive sensitizer. The basic thermal and mechanical properties of these formulations are shown in Table 6. As the percentage of difunctional monomer increases, the T_g and ν_e of the coatings increase correspondently. As a result, poorer laser ablation of the coating (later beginning of ablation, shallower and smaller ablated vias) was found, as shown in Fig. 8. This can be explained by the fact that more energy is needed to break multiple covalent bonds in a more highly crosslinked system to create a via by material removal. Since, a thermal mechanism is inevitably involved in the laser ablation process, it is undoubtedly that T_g, as one of the most important thermal properties of a polymer, will play a role in the ablation process.

The effect of sensitizer NDC-OX on the higher T_g coating

Table 7
Cycloaliphatic epoxide and oxetane conversion for system ECC-EHMO with T_g variation in RTIR experiments

Formulations	Epoxide conv. (%) at 120 s	Oxetane conv. (%) at 120 s
ECC-EHMO blank	46	69
Mid T_g	63	80
Mid T_g+NDC-OX	72	83
High T_g	51	63
High T_g+NDC-OX	67	76

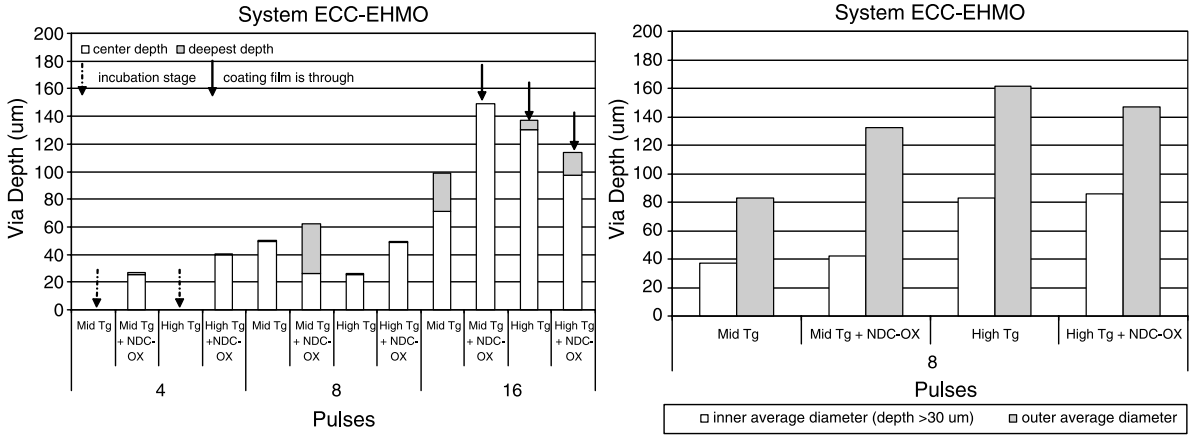

Fig. 9. Dimension data for laser ablation vias of mid and high T_g samples in system ECC-EHMO.

formulations was also examined. The thermal and mechanical properties of these sensitized formulations compared to non-sensitized ones are given in Table 6, and the RTIR and laser ablation results are shown in Table 7 and Fig. 9. In coatings with higher T_g and ν_e, the addition of sensitizer still gives accelerated curing. As a result, increased T_g and ν_e were observed in formulation ECC-EHMO mid T_g+NDC-OX compared to ECC-EHMO mid T_g. For formulation ECC-EHMO high T_g, the T_g is higher than the non-sensitized coating (ECC-EHMO high T_g), but the ν_e is lower, indicating that when the content of difunctional monomer is high enough, boosting the conversion of such monomer may not further increase ν_e due to spatial factors. As to the laser ablation performance, earlier start of ablation, deeper depth and larger diameter of ablated via were also observed for the sensitized coating films. These results further confirm the role of reactive sensitizers in aiding coating curing and laser ablation.

It is apparent that many variables, such as coating composition, T_g, crosslink density and sensitizer addition, factor in the properties of a laser ablatable cationic UV curable coating. Careful optimization of all these variables is necessary in order to develop a successful coating system for a commercial application.

4. Conclusions

Novel reactive sensitizers NDC-OX and ACA-OL were synthesized by reacting naphthalene or anthracene derivatives with EHMO and PCL. These sensitizers had good solubility in cycloaliphatic epoxide based cationic UV curable coatings, consequently the coatings sensitized with ~1 wt% sensitizers exhibit accelerated UV curing, resulting in higher T_g, hardness, and crosslink density. Profile and dimension data (depth and diameter) of vias created by Nd:YAG UV laser ablation on sensitized coating films and Kapton and PEN reference films were obtained. Deeper depth and larger diameter vias were found for sensitized coatings than non-sensitized ones. ACA-OL sensitized coatings have the best laser ablation performance among the tested coating samples due to the stronger and wider absorption of anthracene around 355 nm. ACA-OL sensitized coatings even have deeper laser ablation depth than Kapton, which is a standard laser ablation material. No adverse effect on coating performance was found after addition of reactive sensitizers. The effect of T_g on laser ablation behavior was investigated, and it was found that laser ablation becomes more difficult with higher T_g and ν_e.

Acknowledgements

We thank David Christianson and Shane Stafslien of CNSE for assistance with the GC-MS and HPLC experimentations, and thank Mark Hadley and Scott Herrman of Alien Technology Inc. for the Nd:YAG laser ablation experiments. This material is based on research sponsored by the Defense Microelectronics Activity (DMEA) under Agreements Numbers H94003-04-2-0406, and H94003-06-2-0601. The United States Government is authorized to reproduce and distribute reprints for Government purposes notwithstanding any copyright notation thereon.

References

[1] Sangermano M, Malucelli G, Bongiovanni R, Gozzelino G, Peditto F, Priola A. J Mater Sci 2002;37(22):4753–7.
[2] Koleske JV, Spurr OK, McCarthy NJ. Natl SAMPE Tech Conf 1982;14:249–56.
[3] Koleske JV, McCarthy NJ, Spurr OK. Natl SAMPE Tech Conf 1984;16:529–36.
[4] Holland DL, Tassinari TH, Annu Tech Conf, Soc Plast Eng, Tech Pap, 27th 1969;15:84–89.
[5] Crivello JV, Jiang F. Chem Mater 2002;14:4858–66.
[6] Nelson EW, Carter TP, Scranton AB. Polym Mater Sci Eng 1993;69:363–4.
[7] Cho JD, Kim HK, Kim YS, Hong JW. Polym Test 2003;22:633–45.
[8] Hua Y, Jiang F, Crivello JV. Chem Mater 2002;14:2369–77.
[9] Nuyken O, Dahn U, Wokaun A, Kunz T, Hahn C, Hessel V, et al. Acta Polym 1998;49:427–32.
[10] Kunz T, Stebani J, Ihlemann J, Wokaun A. Appl Phys A 1998;67:347–52.
[11] Ortelli EE, Geiger F, Lippert T, Wei J, Wokaun A. Macromolecules 2000;33:5090–7.
[12] Wee SW, Park SM. Bull Korean Chem Soc 2001;22(8):914–6.
[13] Wang J, Niino H, Yabe A. RIKEN Rev 2001;32:43–6.
[14] Metroke TL, Stesikova E, Dou K, Knobbe ET. Prog Org Coat 2003;46:250–8.
[15] Lippert T. Adv Polym Sci 2004;168:51–246.
[16] Lippert T, Hauer M, Phipps CR, Wokaun A. Appl Phys A 2003;77:259–64.

[17] Nash H, PhD Thesis, North Dakota State University; 2003.
[18] Ouchi I, Hosoi M, Matsumoto F. J Appl Polym Sci 1976;20:1983–7.
[19] Kasapoglu F, Yagci Y. Macromol Rapid Commun 2002;23:567–70.
[20] Crivello JV, Dietliker K. Photosensitizations for free radical, cationic and anionic photopolymerization. 2nd ed. NY: Wiley; 1998.
[21] Crivello JV, Conlon DA, Olson DR, Webb KK. J Rad Cur 1986;13(4):2–6 [also see p. 8–9].
[22] Koleske JV. Polym Paint Colour J 1989;179(4249):796–8 [also see p. 800, 802, 804].
[23] Goldberg D, Eaton RF. Mod Paint Coat 1992;82(12):36 [also see p. 39–40, 42].